

A Systematic Comparison of Second-Order Polarization Propagator Approximation and Equation-of-Motion Coupled Cluster Singles and Doubles C–C, C–N, N–N, C–H, and N–H Spin–Spin Coupling Constants†

Janet E. Del Bene,^{*,‡} Ibon Alkorta,[§] and José Elguero[§]

Department of Chemistry, Youngstown State University, Youngstown, Ohio 44555, and Instituto de Química Médica, CSIC, Juan de la Cierva, 3, E-28006 Madrid, Spain

Received: March 8, 2009; Revised Manuscript Received: April 29, 2009

Ab initio one-, two-, and three-bond C–C, C–N, and N–N spin–spin coupling constants, and one-bond C–H and N–H coupling constants have been computed using two different theoretical methods, SOPPA/(qzp,qz2p) and EOM-CCSD/(qzp,qz2p). Both EOM-CCSD (equation-of-motion coupled cluster singles and doubles) and SOPPA (second-order polarization propagator approximation) coupling constants correlate linearly with experimental data. In the great majority of cases, the computed EOM-CCSD C–C, C–N, N–N, and N–H coupling constants are in better agreement with experimental data than SOPPA values, although both levels of theory provide reasonable estimates of these couplings. EOM-CCSD consistently underestimates one-bond C–H coupling constants by about 10 Hz, and SOPPA values of $^1J(\text{C–H})$ are in better agreement with experimental data. The performance of SOPPA supports its use in future studies of coupling constants involving C, N, and H in larger chemical and biological systems.

Introduction

In previous papers of this series,^{1,2} we carried out systematic comparisons of computed X–Y, X–F, and F–F spin–spin couplings constants for series of molecules with the general formulas H_mXYH_n , for X, Y = ^{13}C , ^{15}N , ^{17}O , and ^{19}F . Included in those studies were molecules with X and Y singly, doubly, and triply bonded, as well as selected fluoro derivatives. The coupling constant calculations were carried out with two different theoretical methods, the second-order polarization propagator approximation (SOPPA) and the equation-of-motion coupled cluster singles and doubles method (EOM-CCSD). However, since the EOM-CCSD method provides a higher-level treatment of electron correlation, our observations that this method usually gives better agreement with experiment were not unexpected. Moreover, it was apparent that SOPPA coupling constants could be significantly in error when coupling involved the more electronegative elements O and F, since electron correlation assumes increased importance in such systems. However, we also observed that there were some couplings for which the performance of SOPPA and EOM-CCSD was similar.

Since SOPPA is a much less expensive computational method, we decided to further evaluate its performance relative to EOM-CCSD and experiment by focusing on coupling involving the less electronegative elements C, N, and H. C–C, C–N, N–N, C–H, and N–H coupling constants can be measured experimentally since all these nuclei have isotopes with spin $I = 1/2$, and are a source of important structural information in chemical and biological systems. Our purpose in the present study is to critique the performance of SOPPA relative to EOM-CCSD and experiment for computing one-, two-, and three-bond coupling constants $^nJ(\text{C–C})$, $^nJ(\text{C–N})$, and $^nJ(\text{N–N})$, and one-bond couplings $^1J(\text{C–H})$ and $^1J(\text{N–H})$. The

results of this study are useful for evaluating the reliability of computed SOPPA coupling constants for future applications to larger chemical and biological systems that are not feasible for EOM-CCSD.

Methods

We have employed experimental geometries for molecules^{3–6} whenever possible in order to minimize the neglect of zero-point vibrational effects on coupling constants.^{2,7} When these were not available, we optimized structures at second-order Møller–Plesset perturbation theory (MP2)^{8–11} with the 6-31+G(d,p) basis set.^{12–15} Vibrational frequencies were computed to confirm that these structures correspond to minima on their potential surfaces. These calculations were carried out with the Gaussian 03 suite of programs.¹⁶

Spin–spin coupling constants involving ^{13}C , ^{15}N , and ^1H were computed using the SOPPA^{17–21} and the EOM-CCSD method in the CI (configuration interaction)-like approximation,^{22,23} with all electrons correlated. Both SOPPA and EOM-CCSD treat explicitly electron correlation effects. SOPPA does this at second-order. Because of its exponential ansatz, EOM-CCSD introduces higher-order terms as products of singles and doubles and thereby provides an improved treatment of electron correlation. All of the coupling constants reported in this paper were obtained with the Ahlrichs²⁴ qzp basis set on ^{13}C and ^{15}N and the qz2p basis set on ^1H . Thus, the levels of theory may be represented as EOM-CCSD/(qzp,qz2p) and SOPPA/(qzp,qz2p). In the Ramsey approximation,²⁵ the total coupling constant (J) is a sum of four contributions: the paramagnetic spin–orbit (PSO), diamagnetic spin–orbit (DSO), Fermi contact (FC), and spin–dipole (SD). All terms have been computed for all molecules. SOPPA calculations were performed using Dalton-2²⁶ on the IQM computers, and the EOM-CCSD calculations were done with ACES II²⁷ on the Itanium Cluster at the Ohio Supercomputer Center.

† Part of the “Russell M. Pitzer Festschrift”.

* Corresponding author, jedelbene@ysu.edu.

‡ Department of Chemistry, Youngstown State University.

§ Instituto de Química Médica, CSIC.

TABLE 1: SOPPA, EOM-CCSD, and Experimental C–C, C–N, N–N, C–H, and N–H Coupling Constants (Hz)^a

no./molecule	coupling	SOPPA	EOM-CCSD	exptl	no./molecule	coupling	SOPPA	EOM-CCSD	exptl
1 CH ₄ ^b	¹ J(C–H)	125.3	117.8	125.31 ^c	19 pyridine	¹ J(N1–C2)	0.9	0.5	0.67 ^k
2 C ₂ H ₆ ^b	¹ J(C–C)	37.7	34.6	34.6 ^d		² J(N1–C3)	3.4	2.9	2.53 ^k
	¹ J(C–H)	124.8	117.3	124.9 ^d		³ J(N1–C4)	–4.5	–3.9	–3.85 ^k
3 (CH ₃) ₂ CH ₂	¹ J(C–C)	39.0	36.0	34.6 ^d		¹ J(C2–C3)	60.9	58.2	54.3 ^d
	² J(C–C)	–2.1	–1.4			¹ J(C3–C4)	60.9	57.8	53.7 ^d
CH ₂	¹ J(C–H)	124.1	116.5	125.4 ^d		² J(C2–C4)	–4.6	–3.3	–2.868 ^m
methyl	¹ J(C–H)	123.1	115.8	124.4 ^d		² J(C2–C6)	–8.9	–7.1	
4 (CH ₃) ₃ CH	¹ J(C–C)	39.1	36.4			² J(C3–C5)	–5.2	–3.6	
	² J(C–C)	–1.2	–0.5			³ J(C2–C5)	16.0	14.1	13.942 ^m
C–H	¹ J(C–H)	125.2	117.5		20 pyrazine	¹ J(N1–C2)	1.4	0.7	
methyl	¹ J(C–H)	122.9	115.5	124.0 ^d		² J(N1–C3)	2.2	2.1	
5 C(CH ₃) ₄	¹ J(C–C)	39.7	36.7	36.9 ^e		³ J(N1–N4)	2.5	1.8	
	² J(C–C)	0.0	0.7			¹ J(C2–C3)	59.9	58.0	
methyl	¹ J(C–H)	123.0	115.7	123.3 ^d		² J(C2–C6)	–9.1	–7.4	
6 cyclopropane ^f	¹ J(C–C)	14.6	13.2	12.4 ^d		³ J(C2–C5)	20.6	18.2	
	¹ J(C–H)	161.0	151.8	160.3 ^d		¹ J(C–H)	184.2	171.7	182.7 ^d
7 C ₂ H ₄ ^b	¹ J(C–C)	75.0	71.1	67.6 ^d	21 1,3,5-triazine	¹ J(N1–C2)	5.0	3.8	
	¹ J(C–H)	160.0	149.0	156.4 ^d		² J(N1–N3)	–0.2	–0.2	
8 H ₂ C=C=CH ₂ ^b	¹ J(C–C)	111.6	105.4	98.7 ^d		³ J(N1–C4)	–6.8	–6.1	
	² J(C–C)	6.5	9.4			² J(C2–C6)	–7.8	–6.8	
	¹ J(C–H)	172.8	159.0	167.8 ^d		¹ J(C–H)	209.1	195.1	207.5 ^d
9 furan ^b	¹ J(C2–C3)	78.5	76.0	69.1 ^d	22 1,2,4,5-tetrazine	¹ J(N1–N2)	–29.9	–24.6	
	¹ J(C3–C4)	56.6	52.8			² J(N1–C3)	2.5	2.7	
	² J(C2–C4)	–0.6	0.8			³ J(N1–N4)	7.6	4.2	
	² J(C2–C5)	3.9	3.6			¹ J(N2–C3)	12.8	11.0	
	¹ J(C2–H)	203.6	190.1	201.8 ^d		² J(N2–N4)	4.8	2.1	
	¹ J(C3–H)	176.9	165.4	174.7 ^d		³ J(C3–C6)	36.0	31.7	
10 benzene ^b	¹ J(C1–C2)	63.1	60.3	55.9 ^g		¹ J(C–H)	212.8	198.3	213.2 ⁿ
	² J(C1–C3)	–4.4	–2.8	–2.46 ^g	23 N ₂ ^h	¹ J(N–N)	–4.8	–3.1	–2.5 ^k
	³ J(C1–C4)	11.6	10.1	10.05 ^g	24 N ₃ H ^o	¹ J(N1–N2)	–18.0	–14.6	–13.95 ^k
	¹ J(C–H)	160.7	149.7	158.4 ^d		¹ J(N2–N3)	–10.8	–7.4	–7.2 ^k
11 HC≡CH ^h	¹ J(C–C)	198.6	194.9	174.8 ⁱ		² J(N1–N3)	–1.2	–0.8	
	¹ J(C–H)	259.8	240.0	249.0 ^d		¹ J(N1–H)	–75.1	–74.0	–70.2 ^k
12 (CH ₃)C≡CH ^b	¹ J(C≡C)	197.6	193.7		25 H ₃ C–CN ^b	¹ J(C–N)	–13.5	–16.6	–16.2 ^l
	¹ J(C–C)	72.5	68.0	67.4 ^s		¹ J(C–C)	67.1	63.8	60.12 ^l
	² J(C–C)	12.2	13.1	11.8 ^e		² J(C–N)	3.6	3.0	2.9 ^p
C–H triple	¹ J(C–H)	257.7	238.1	248.1 ^d		¹ J(C–H)	137.1	127.5	134.0 ^l
methyl	¹ J(C–H)	135.4	125.8	131.6 ^d	26 NH ₄ ⁺	¹ J(N–H)	–76.8	–73.5	–73.3 ^k
13 NH ₃	¹ J(N–H)	–63.9	–61.5	–61.4 ⁱ	27 (CH ₃)NH ₃ ⁺	¹ J(C–N)	–4.4	–3.8	<8 ^q
14 (CH ₃)NH ₂	¹ J(C–N)	–6.3	–5.7	–4.5 ^k		¹ J(C–H)	149.6	140.7	145 ^q
	¹ J(C–H)	131.2	123.1	133 ^d		¹ J(N–H)	–77.9	–74.5	–74.92 ^q
	¹ J(N–H)	–66.2	–63.5	–64.5 ^k	28 (CH ₃) ₂ NH ₂ ⁺	¹ J(C–N)	–5.7	–5.0	
15 (CH ₃) ₂ NH	¹ J(C–N)	–6.8	–6.1			² J(C–C)	–1.0	–0.6	
	² J(C–C)	–2.3	–1.6			¹ J(C–H)	147.0	138.2	
	¹ J(C–H)	130.7	122.7			¹ J(N–H)	–78.1	–74.6	–76.53 ^q
	¹ J(N–H)	–70.3	–67.5	–67.0 ^k	29 (CH ₃) ₃ NH ⁺	¹ J(C–N)	–6.7	–5.8	
16 N(CH ₃) ₃	¹ J(C–N)	–5.8	–5.1			² J(C–C)	–0.5	–0.1	
	² J(C–C)	–1.8	–1.1			¹ J(C–H)	145.3	136.3	143 ^q
	¹ J(C–H)	130.7	122.8	131.5 ^j		¹ J(N–H)	–78.7	–75.1	–76.7 ^q
17 H ₂ C=NH	¹ J(C–N)	–1.5	–1.9		30 (CH ₃) ₄ N ⁺	¹ J(C–N)	–7.2	–6.4	–5.5 ^q
	¹ J(N–H)	–49.4	–46.8			² J(C–C)	0.0	0.4	
cis to N–H	¹ J(C–H)	160.9	150.5			¹ J(C–H)	144.3	135.7	145 ^q
trans to N–H	¹ J(C–H)	176.3	164.7		31 pyridinium	¹ J(N1–C2)	–15.6	–14.7	–12.0 ^k
18 pyrrole	¹ J(N1–C2)	–16.7	–16.1	–12.98 ^k		² J(N1–C3)	2.7	1.9	2.01 ^k
	² J(N1–C3)	–4.4	–4.6	–3.92 ^k		³ J(N1–C4)	–6.2	–5.5	–5.3 ^k
	¹ J(C2–C3)	74.1	71.5	–65.6 ^d		¹ J(C2–C3)	66.0	63.0	
	¹ J(C3–C4)	61.9	58.7			¹ J(C3–C4)	58.2	55.3	
	² J(C2–C4)	0.3	1.6			² J(C2–C4)	–3.9	–3.0	
	¹ J(C2–H)	187.9	175.4	183.3 ^d		² J(C2–C6)	–5.2	–4.2	
	¹ J(C3–H)	173.0	161.7	168.8 ^d		² J(C3–C5)	–4.1	–2.7	
	¹ J(N–H)	–98.1	–93.4	96.5 ^k		³ J(C2–C5)	9.8	8.8	
						¹ J(N–H)	–98.3	–93.3	–90.5 ^k

^a Geometries are optimized MP2/6-31+G(d,p) geometries except where noted; ¹J(C–H) for methyl C–H couplings is the weighted average.

^b Geometry from ref 3. ^c Reference 28. ^d Reference 29. ^e Reference 30. ^f Geometry from ref 4. ^g Reference 31. ^h Geometry from ref 5. ⁱ Reference 32. ^j Reference 33. ^k Reference 34. ^l Reference 35. ^m Reference 36. ⁿ Reference 37. ^o Geometry from ref 6. ^p Reference 38. ^q Reference 39.

Results and Discussion

Seventy-one experimentally measured coupling constants^{28–39} have been reported for the 31 molecules included in this study. These molecules are listed by number in Table 1, beginning with

CH₄ and followed by molecules with C–C single, double, and triple bonds. The molecule furan has also been included in this section. These 12 molecules are followed by NH₃ and 9 neutral molecules containing C–N single and double bonds, and then 3

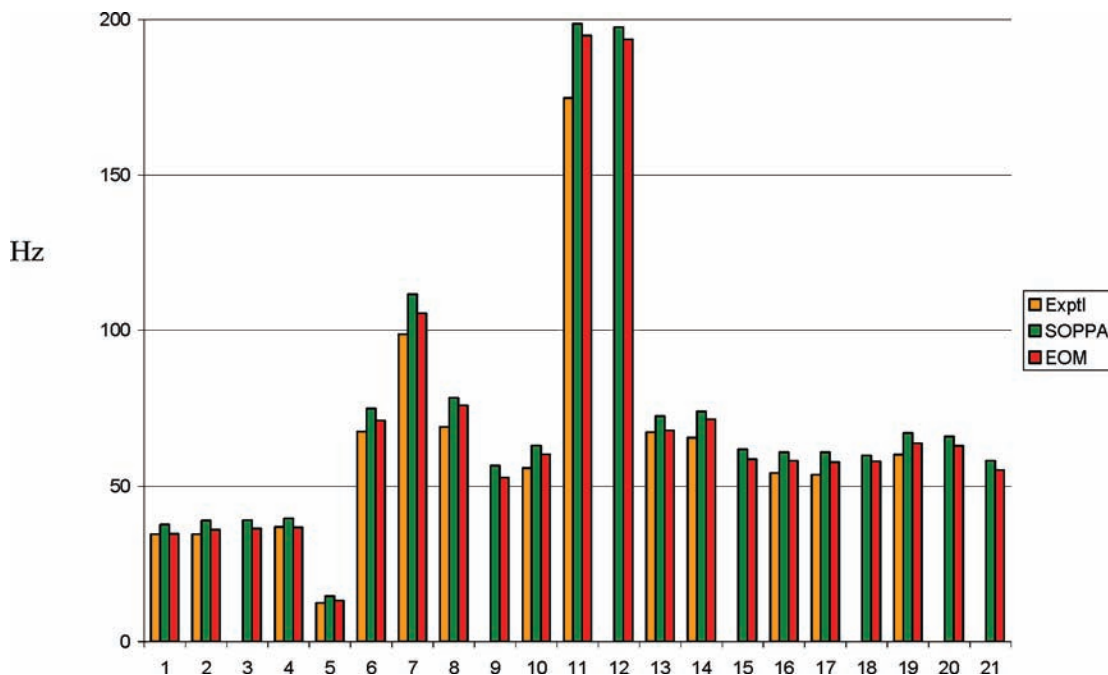


Figure 1. Bar graph comparing SOPPA, EOM-CCSD, and experimental $^1J(\text{C}-\text{C})$ values.

molecules with either C–N or N–N triple bonds. The final six entries are the cations NH_4^+ and its methyl derivatives and pyridinium. Table S1 of the Supporting Information lists the individual terms which contribute to the total coupling constants.

Coupling constants for many of the small molecules investigated in this study have been computed by others using various methods, basis sets, and geometries.^{40–45} However, it is our purpose in the present study to compare coupling constants computed with two different theoretical methods, both of which explicitly treat electron correlation effects, using the same geometry and the same basis set. Thus, our focus is on similarities or differences which can be directly attributed to the two different methodologies, SOPPA and EOM-CCSD.

Some limitations of our treatment of the experimental data should be noted. If more than one experimental value of a particular coupling constant has been reported for a molecule, we have used that one judged to be the most reliable. No adjustments have been made for uncertainties in the experimental assignments or for reported error bars. Finally, we have not taken into account the fact that the experimental coupling constants have been measured under different conditions, some in the gas phase and others in solution, and no adjustments have been made to account for possible interactions between the solute and the solvent. It is not possible to state in general the extent to which phase changes or solute–solvent interactions influence coupling constants, since such changes depend on the nature of the species, changes in molecular geometry, or the strength of the interaction of the species with the solvent. Suffice it to say that if the interaction is strong, as might be the case if a relatively strong hydrogen bond were formed, such effects could be appreciable.^{46,47} The very good agreement between theory and experiment which will be evident below suggests that for the molecules investigated in this study such effects do not appear to have a dominant influence.

C–C Coupling Constants. There are 48 one-, two-, and three-bond C–C coupling constants reported in Table 1, with experimental data available for 19 of these. The majority of these couplings are one-bond C–C couplings. Analysis of these data is facilitated by bar graphs and plots which compare corresponding SOPPA, EOM-CCSD, and experimental values.

One-Bond C–C Couplings. Figure 1 presents a bar graph showing 21 computed SOPPA and EOM-CCSD one-bond C–C coupling constants together with 14 corresponding experimentally measured values. The numbering in Figure 1 follows the listing of coupling constants in Table 1. It is apparent from Figure 1 that all one-bond C–C coupling constants are positive, ranging from about 10 Hz for molecule **6** (cyclopropane) to about 200 Hz for **11** and **12** ($\text{HC}\equiv\text{CH}$ and $\text{H}_3\text{C}-\text{C}\equiv\text{CH}$). SOPPA coupling constants are always greater than those of EOM-CCSD, with the latter in better agreement with experiment. With one EOM-CCSD exception, both EOM-CCSD and SOPPA coupling constants overestimate experimental $^1J(\text{C}-\text{C})$ values, with the largest error occurring for $\text{HC}\equiv\text{CH}$.²

Figure 2 presents a plot of SOPPA and EOM-CCSD $^1J(\text{C}-\text{C})$ values versus the corresponding experimental values. Also shown in Figure 2 for comparison is a reference trendline which has a slope of 1 and an intercept of 0.0 Hz. The equations of the EOM-CCSD and SOPPA trendlines are

$$^1J(\text{EOM-CCSD}) = 1.12 \ ^1J(\text{exptl}) - 3.47$$

$$n = 14; R^2 = 0.998 \quad (1)$$

$$^1J(\text{SOPPA}) = 1.14 \ ^1J(\text{exptl}) - 1.12$$

$$n = 14; R^2 = 0.999 \quad (2)$$

Thus, it is apparent that both SOPPA and EOM-CCSD correlate linearly with experimental data, with the trendline for EOM-CCSD closer to the reference trendline. However, the slopes of both trendline are too high, reflecting the tendency of both methods to overestimate one-bond C–C coupling constants. A plot in which $^1J(\text{C}-\text{C})$ for the worst case ($\text{HC}\equiv\text{CH}$) is omitted only slightly reduces the slopes of the EOM-CCSD (1.09) and SOPPA (1.13) trendline.

Two- and Three-Bond C–C Couplings. Figure 3 presents a bar graph showing the 22 SOPPA and EOM-CCSD two-bond C–C coupling constants $^2J(\text{C}-\text{C})$. The two-bond couplings are rather small, ranging from about -10 to $+15$ Hz. Computed EOM-CCSD $^2J(\text{C}-\text{C})$ values are more positive

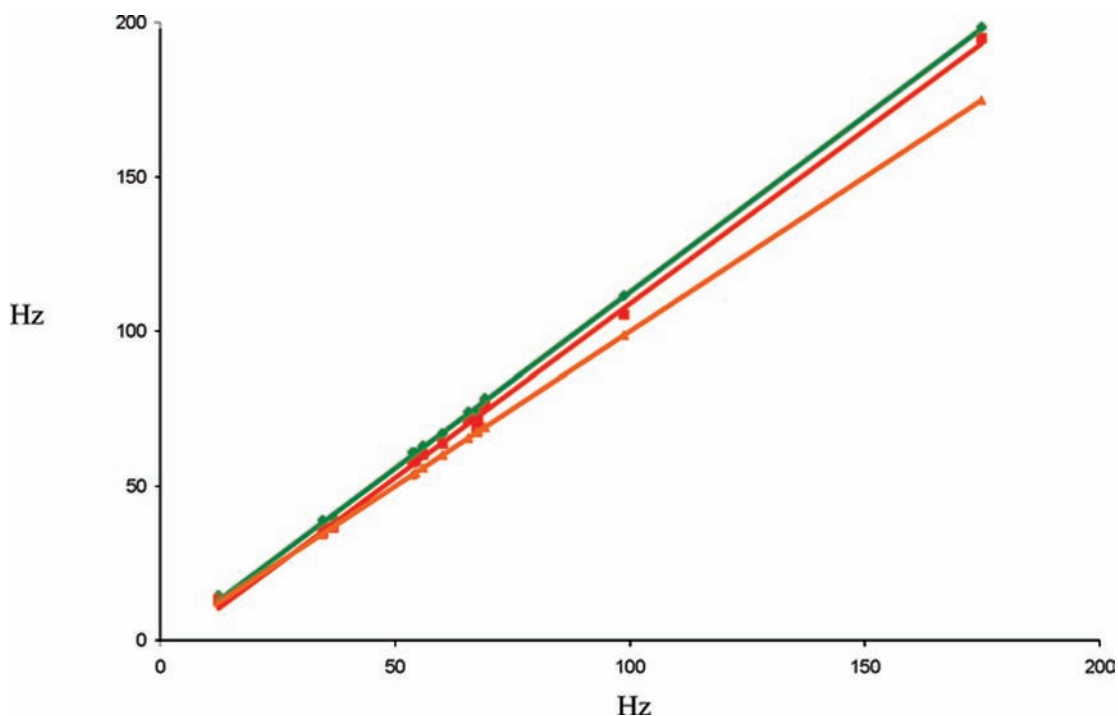


Figure 2. SOPPA (◆, green line) and EOM-CCSD (■, red line) $^1J(\text{C}-\text{C})$ vs experimental values and the reference trendline (▲, orange line).

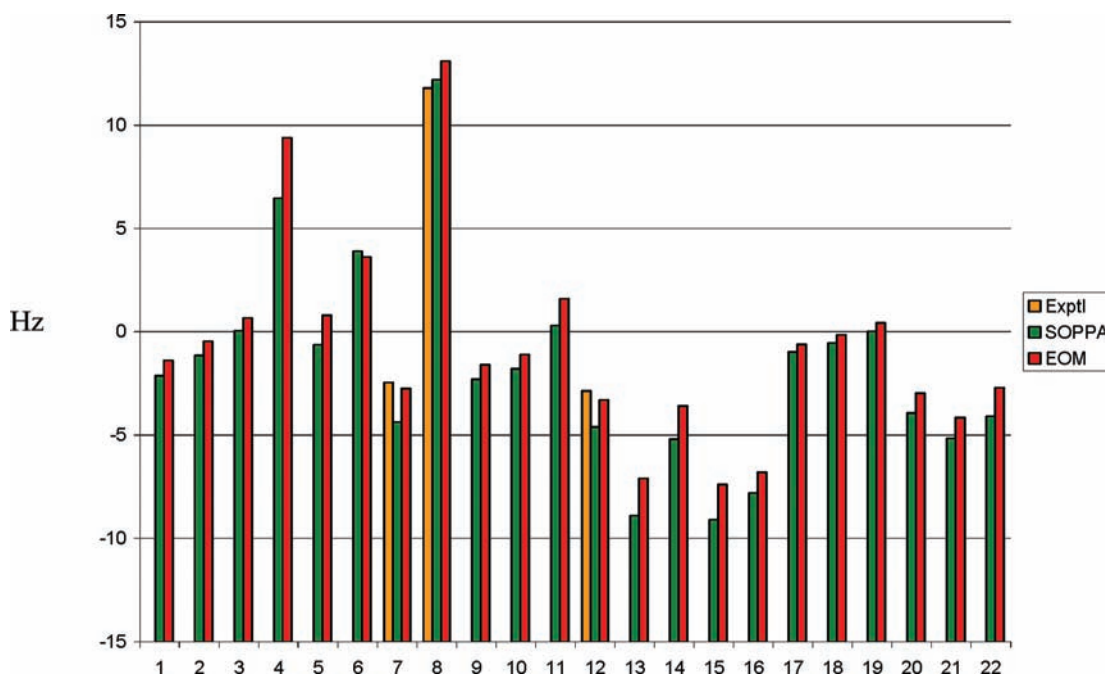


Figure 3. Bar graph comparing SOPPA, EOM-CCSD, and experimental $^2J(\text{C}-\text{C})$ values.

than corresponding SOPPA values, except for $^2J(\text{C}2-\text{C}5)$ in furan, in which case the SOPPA value is slightly greater (3.9 vs 3.6 Hz). There are only three experimental coupling constants available for comparison. When two-bond coupling occurs in the aromatic molecules **10** (benzene) and **19** (pyridine), $^2J(\text{C}-\text{C})$ is small and negative and EOM-CCSD is in closer agreement with experiment. The two-bond coupling constant in molecule **12** ($\text{H}_3\text{C}-\text{C}\equiv\text{CH}$) is positive and SOPPA is in better agreement with experiment.

There are only five three-bond couplings $^3J(\text{C}-\text{C})$, which range from about 10 to 35 Hz, and these are always greater at SOPPA compared to EOM-CCSD. Only two of these have been measured experimentally, and in both **10** and **19**, the

EOM-CCSD values are in better agreement with experiment, as evident from Table 1. A plot of the computed EOM-CCSD and SOPPA $^2J(\text{C}-\text{C})$ and $^3J(\text{C}-\text{C})$ values versus the experimental coupling constants is shown in Figure 4. This plot illustrates once again the tendency of SOPPA to overestimate absolute values of C-C coupling constants, as indicated by the slope of the SOPPA trendline. The equations of these lines are

$$^nJ(\text{EOM-CCSD}) = 1.06 ^nJ(\text{exptl}) - 1.19$$

$$n = 5; R^2 = 0.997 \quad (3)$$

$${}^nJ(\text{SOPPA}) = 1.21 {}^nJ(\text{exptl}) - 1.23$$

$$n = 5; R^2 = 0.997 \quad (4)$$

for ${}^nJ(\text{C}-\text{C})$ including both ${}^2J(\text{C}-\text{C})$ and ${}^3J(\text{C}-\text{C})$. Both EOM-CCSD and SOPPA coupling constants correlate linearly with experimental data, with the EOM-CCSD and reference trendlines nearly superimposable.

C-N Coupling Constants. There are 24 one-, two-, and three-bond C-N coupling constants reported in Table 1. Experimental data are available for six of the one-bond couplings, four two-bond couplings, and two three-bond couplings.

One-Bond C-N Couplings. Figure 5 presents a bar graph comparing the EOM-CCSD, SOPPA, and experimental one-bond C-N coupling constants. Bars labeled 1-3, 5, and 11-14 refer to C-N single bonds in neutral molecules and ions. For these and the C-N bond in pyridinium (bar 15), ${}^1J(\text{C}-\text{N})$ is negative, with the absolute value of the SOPPA coupling constant greater than EOM-CCSD. Bars 4 and 10 represent the double bond in **17** ($\text{H}_2\text{C}=\text{NH}$) and the triple bond in **25** ($\text{H}_3\text{C}-\text{C}\equiv\text{N}$), respectively. These one-bond couplings are also negative, with the absolute value of the EOM-CCSD coupling constant greater than SOPPA. Bars 6-9 are one-bond C-N

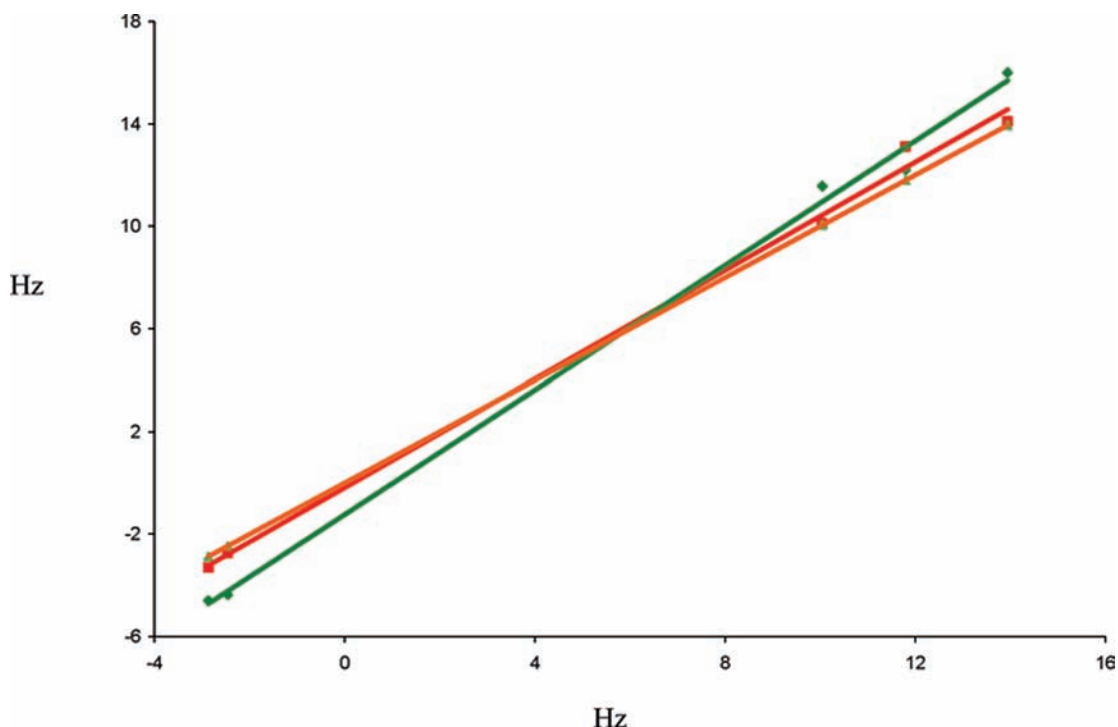


Figure 4. SOPPA (♦, green line) and EOM-CCSD (■, red line) ${}^2J(\text{C}-\text{C})$ and ${}^3J(\text{C}-\text{C})$ vs experimental values and the reference trendlines (▲, orange line).

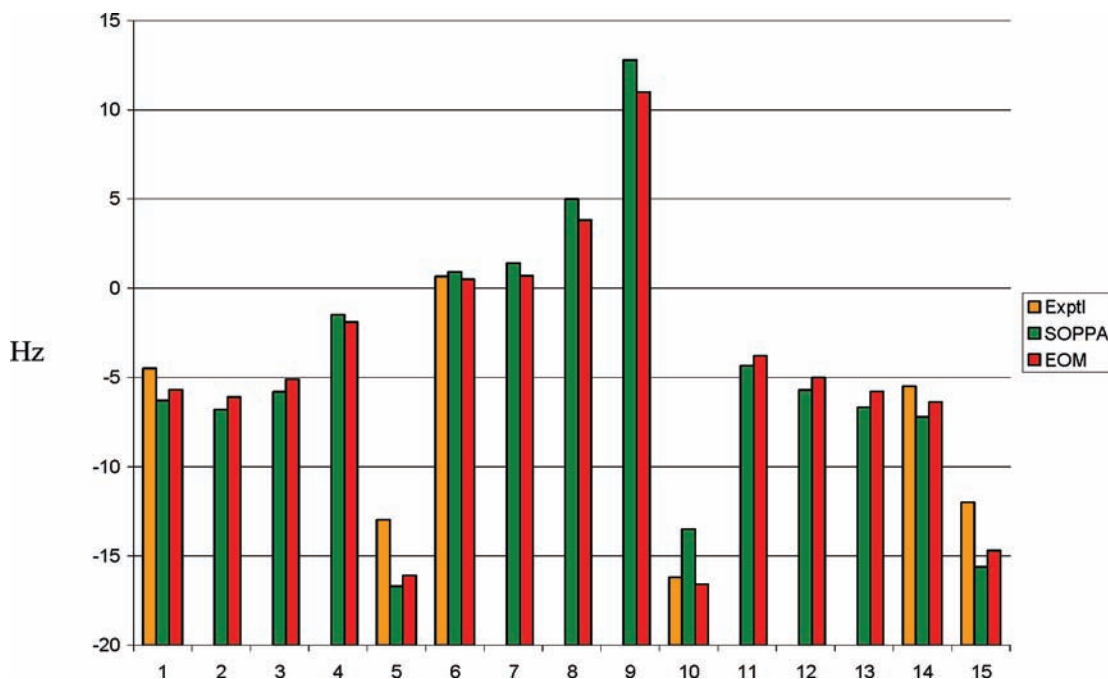


Figure 5. Bar graph comparing SOPPA, EOM-CCSD, and experimental ${}^1J(\text{C}-\text{N})$ values.

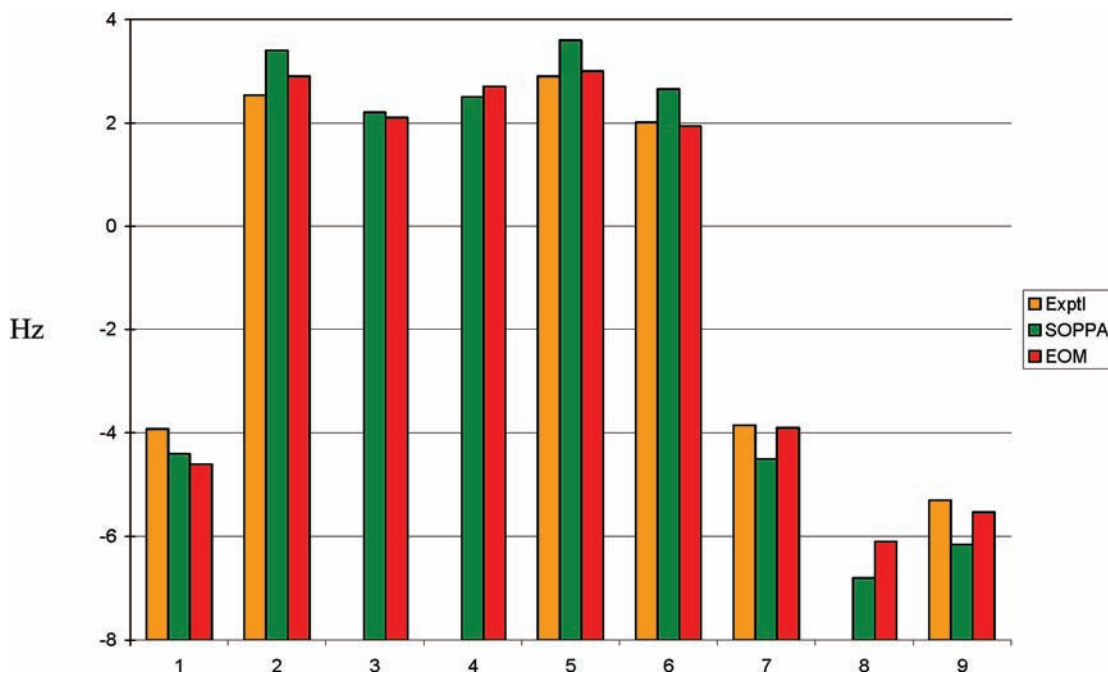


Figure 6. Bar graph comparing SOPPA, EOM-CCSD, and experimental ${}^2J(\text{C}-\text{N})$ (bars 1–6) and ${}^3J(\text{C}-\text{N})$ (bars 7–9) values.

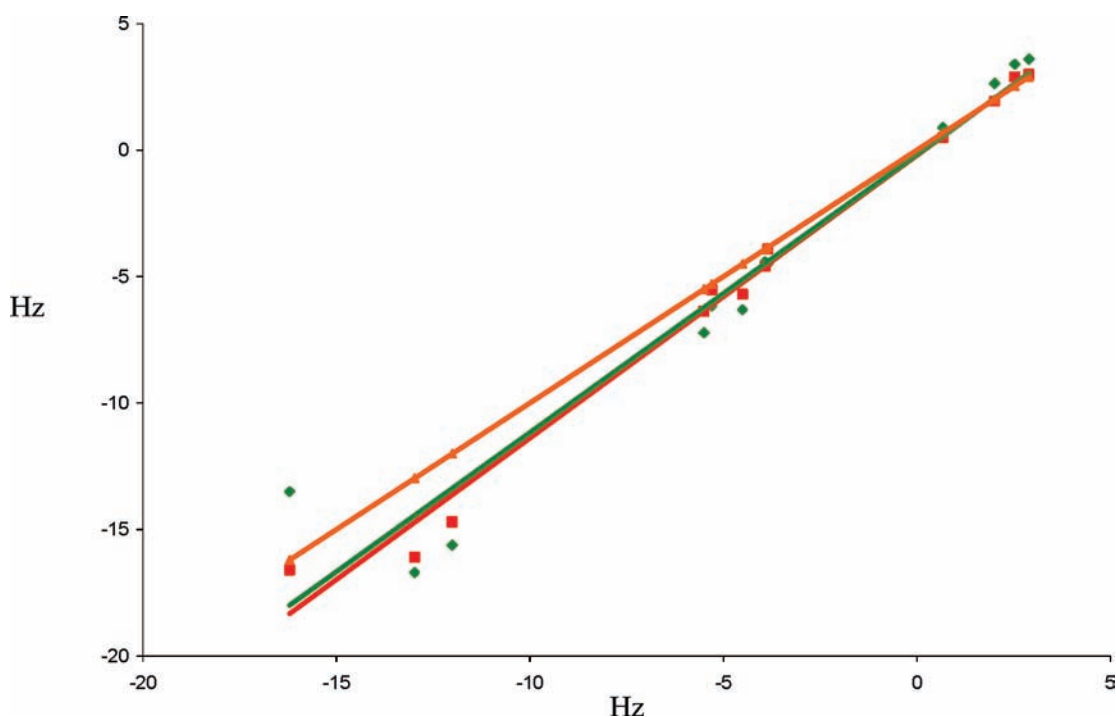


Figure 7. SOPPA (\blacklozenge , green line) and EOM-CCSD (\blacksquare , red line) ${}^1J(\text{C}-\text{N})$, ${}^2J(\text{C}-\text{N})$, and ${}^3J(\text{C}-\text{N})$ vs experimental values and the reference trendline (\blacktriangle , orange line).

couplings in the azabenzene. These coupling constants are positive, with the SOPPA values greater than EOM-CCSD. It is also apparent from this figure that although the EOM-CCSD values are in better agreement with experiment, both methods yield similar coupling constants. The largest difference is found for $\text{H}_3\text{C}-\text{C}\equiv\text{N}$, in which case the absolute value of the SOPPA coupling constant is 3.1 Hz less than that of EOM-CCSD and underestimates the experimental value by 2.7 Hz. Both SOPPA and EOM-CCSD overestimate the absolute value of ${}^1J(\text{C}-\text{N})$ for **18** (pyrrole) by 4 and 3 Hz, respectively.

Two and Three-Bond C–N Couplings. Figure 6 presents a bar graph comparing computed and experimental two-bond (bars 1–6) and three-bond (bars 7–9) C–N coupling constants.

${}^2J(\text{C}-\text{N})$ values from the azabenzene, pyridinium, and $\text{H}_3\text{C}-\text{C}\equiv\text{N}$ are small and positive, while ${}^2J(\text{C}-\text{N})$ for pyrrole is small and negative. The three-bond C–N couplings are also negative at both levels of theory. Experimental data are available for six of these nine coupling constants, and for all except ${}^2J(\text{C}-\text{N})$ in pyrrole, EOM-CCSD is in better agreement with experiment. Figure 7 presents a plot of SOPPA and EOM-CCSD one-, two-, and three-bond C–N coupling constants versus the experimental values. The equations of the trendlines are

$${}^nJ(\text{EOM-CCSD}) = 1.12 {}^nJ(\text{exptl}) - 0.20$$

$$n = 12; R^2 = 0.987 \quad (5)$$

$${}^nJ(\text{SOPPA}) = 1.10 {}^nJ(\text{exptl}) - 0.17$$

$$n = 12; R^2 = 0.940 \quad (6)$$

The computed values of the C–N coupling constants at the two levels of theory agree with each other better than they agree with experiment, and the slopes of the trendlines are too high. As evident from Figure 6, both methods overestimate the absolute values of ${}^1J(\text{C–N})$ for pyrrole and pyridinium, but SOPPA also underestimates the absolute value of ${}^1J(\text{C–N})$ for $\text{H}_3\text{CC}\equiv\text{N}$, which leads to a lowering of the SOPPA correlation coefficient. However, none of the computed values is unreasonable.

N–N Coupling Constants. There are only nine one-, two-, and three-bond N–N coupling constants in the set of molecules and ions included in this study, and experimental data are available for only three one-bond N–N couplings. The values of these coupling constants are represented in the bar graph of Figure 8. Bars 1 and 3 are one-bond couplings across N–N single bonds, while bars 2 and 4 are one-bond couplings across N–N triple bonds. The absolute values of the SOPPA coupling constants are greater than the EOM-CCSD coupling constants, and both overestimate the experimental values, although EOM-CCSD ${}^1J(\text{N–N})$ values are in better agreement with experiment. The two-bond couplings are essentially zero in **21** (1,3,5-triazine), positive in **22** (1,2,4,5-tetrazine), and negative in **24** (N_3H). The three-bond couplings in **20** (pyrazine) and **22** are positive, with the SOPPA values greater than those of EOM-CCSD.

C–H Coupling Constants. There are 31 one-bond C–H coupling constants in the molecules and ions included in this study, with experimental values available for 26 of these. Figure 9 provides a comparison of EOM-CCSD, SOPPA, and experimental data. It is apparent from this figure that C–H coupling constants are always positive and range from about 100 to 250 Hz. For these C–H couplings, SOPPA values are always greater than those of EOM-CCSD and are in better agreement with experimental values. As evident from Figure 9 and Table 1,

the computed EOM-CCSD coupling constants underestimate experimental C–H coupling constants by about 10 Hz. This is the only case found in this and our previous studies in which the performance of SOPPA is superior to that of EOM-CCSD. The better agreement between SOPPA and experimental C–H coupling constants can also be seen in Figure 10, which shows a plot of EOM-CCSD and SOPPA coupling constants versus experimental values. A reference point at (0,0) has been added for both methods. The equations of the trendlines are

$${}^1J(\text{EOM-CCSD}) = 0.96 {}^1J(\text{exptl}) - 2.03$$

$$n = 26; R^2 = 0.998 \quad (7)$$

$${}^1J(\text{SOPPA}) = 1.03 {}^1J(\text{exptl}) - 3.36$$

$$n = 26; R^2 = 0.996 \quad (8)$$

Although statistically there appears to be little difference between the two methods, the SOPPA trendline can be seen to lie almost on top of the reference trendline.

N–H Coupling Constants. Experimental coupling constants have been measured for 10 of the 11 one-bond N–H couplings found in the molecules and ions included in this study. These are illustrated for comparative purposes in Figure 11. All one-bond N–H coupling constants are negative and range from about –50 to –100 Hz. The absolute values of SOPPA coupling constants are always greater by about 5 Hz than the corresponding EOM-CCSD coupling constants, with the latter usually in better agreement with experiment. Figure 12 provides a plot of EOM-CCSD and SOPPA versus experimental N–H coupling constants. A reference point at (0,0) has been added for both methods. The trendline equations are

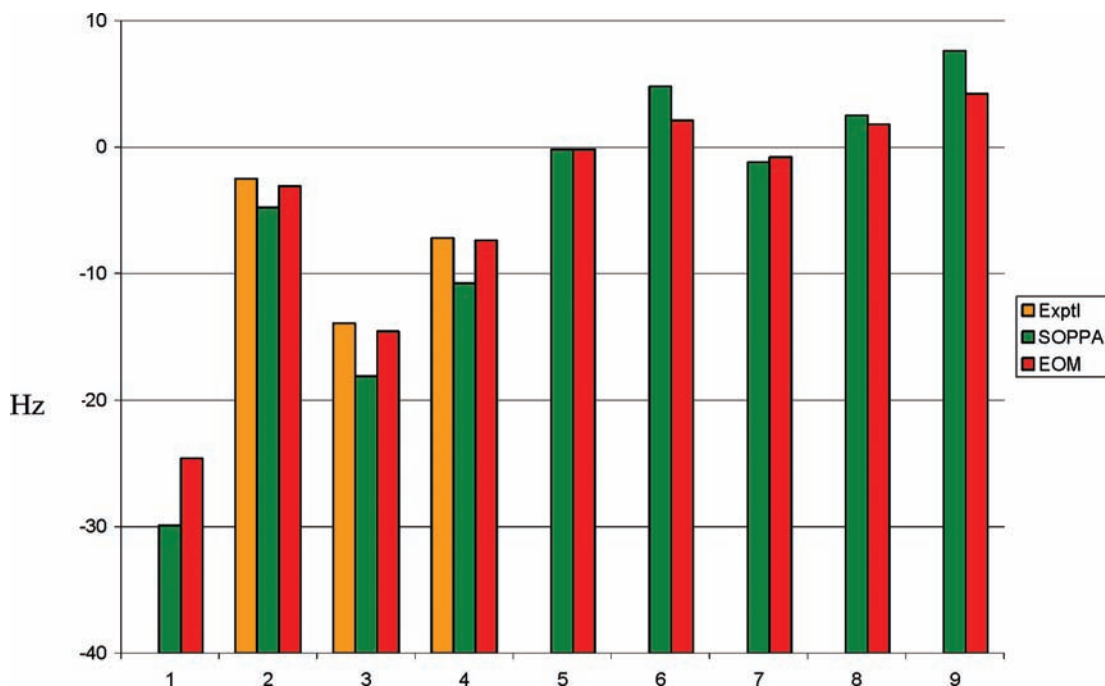


Figure 8. Bar graph comparing SOPPA, EOM-CCSD, and experimental ${}^1J(\text{N–N})$, ${}^2J(\text{N–N})$, and ${}^3J(\text{N–N})$ values. Bars 1–4 arise from coupling across N–N single bonds; bars 5–7 correspond to coupling across N–N double bonds; bars 8 and 9 correspond to coupling across N–N triple bonds.

$${}^1J(\text{EOM-CCSD}) = 0.99 {}^1J(\text{exptl}) - 0.79$$

$$n = 10; R^2 = 0.993 \quad (9)$$

$${}^1J(\text{SOPPA}) = 1.04 {}^1J(\text{exptl}) - 0.19$$

$$n = 10; R^2 = 0.995 \quad (10)$$

For these one-bond N–H couplings, the EOM-CCSD and reference trendlines are essentially superimposable.

Conclusions

C–C, C–N, N–N, C–H, and N–H spin–spin coupling constants have been computed using two different theoretical

methods, SOPPA/(qzp,qz2p) and EOM-CCSD/(qzp,qz2p), both of which explicitly treat electron correlation effects. The computed values have been compared with each other and with experimental data. The following statements are supported by the results of this study.

1. Both EOM-CCSD and SOPPA overestimate one-bond C–C couplings. The SOPPA values are greater than those of EOM-CCSD, with the latter being in better agreement with experiment. One-, two-, and three-bond EOM-CCSD and SOPPA C–C coupling constants correlate linearly with experimental values, with EOM-CCSD usually in better agreement with experiment.

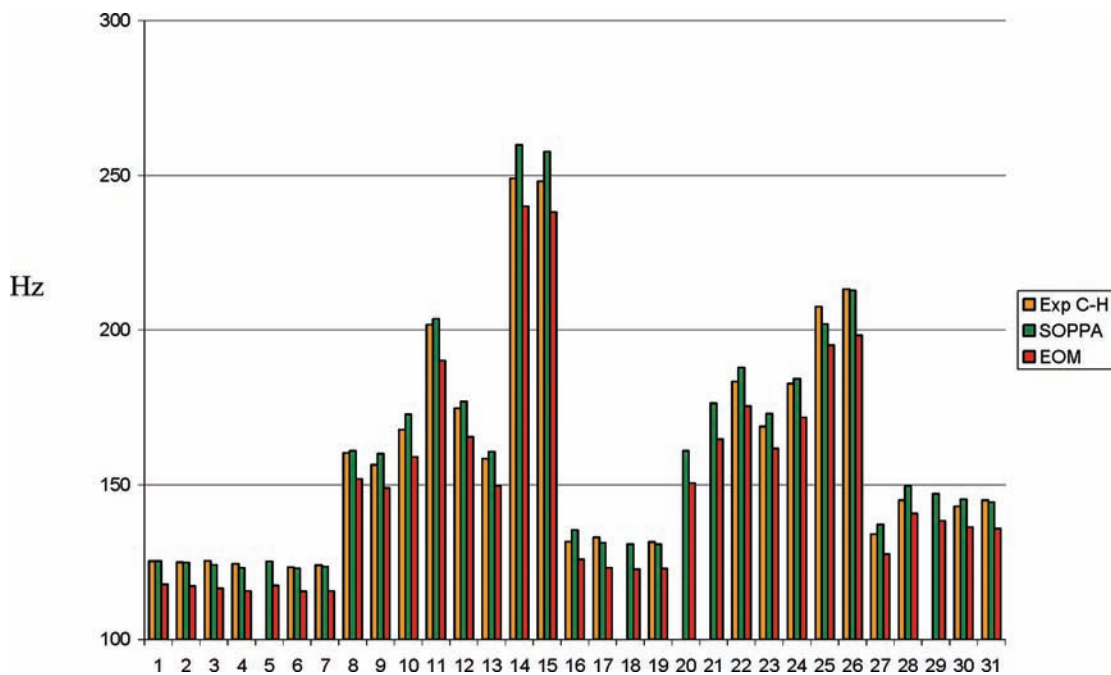


Figure 9. Bar graph comparing SOPPA, EOM-CCSD, and experimental ${}^1J(\text{C-H})$ coupling constants.

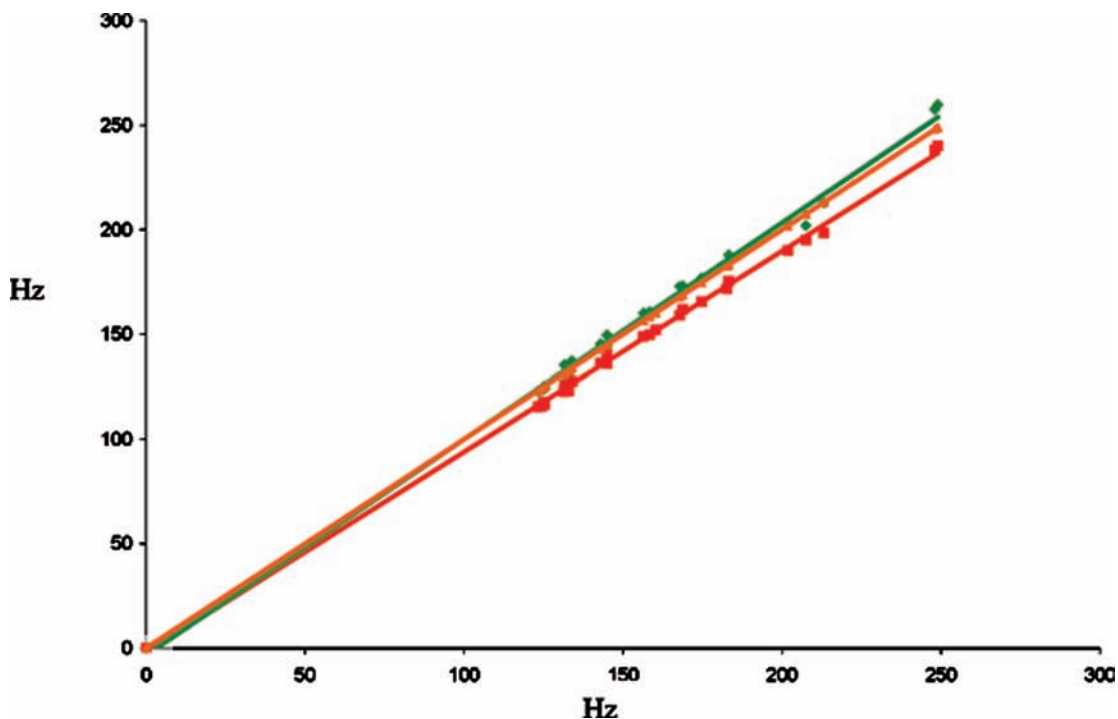


Figure 10. SOPPA (\blacklozenge , green line) and EOM-CCSD (\blacksquare , red line) ${}^1J(\text{C-H})$ vs experimental values and the reference trendline (\blacktriangle , orange line). A point at (0,0) has been added for both methods.

2. Although one-bond EOM-CCSD C–N coupling constants are in better agreement with experimental data, the computed values at the two levels of theory are similar. Moreover, computed two- and three-bond C–N coupling constants at the two levels of theory are in better agreement with each other than with experimental data, although both correlate linearly with experiment.

3. One-, two-, and three-bond N–N coupling constants computed at EOM-CCSD and SOPPA are similar, with the EOM-CCSD values usually in better agreement with experimental data.

4. SOPPA one-bond C–H coupling constants are in better agreement with experimental values than EOM-CCSD. The EOM-CCSD coupling constants underestimate $^1J(\text{C–H})$ by about 10 Hz.

5. The absolute values of one-bond SOPPA N–H coupling constants are about 5 Hz greater than EOM-CCSD values, with the latter usually in better agreement with experimental data.

6. Both EOM-CCSD and SOPPA provide good estimates of coupling constants involving C, N, and H. The performance of SOPPA supports its use in future studies of couplings involving

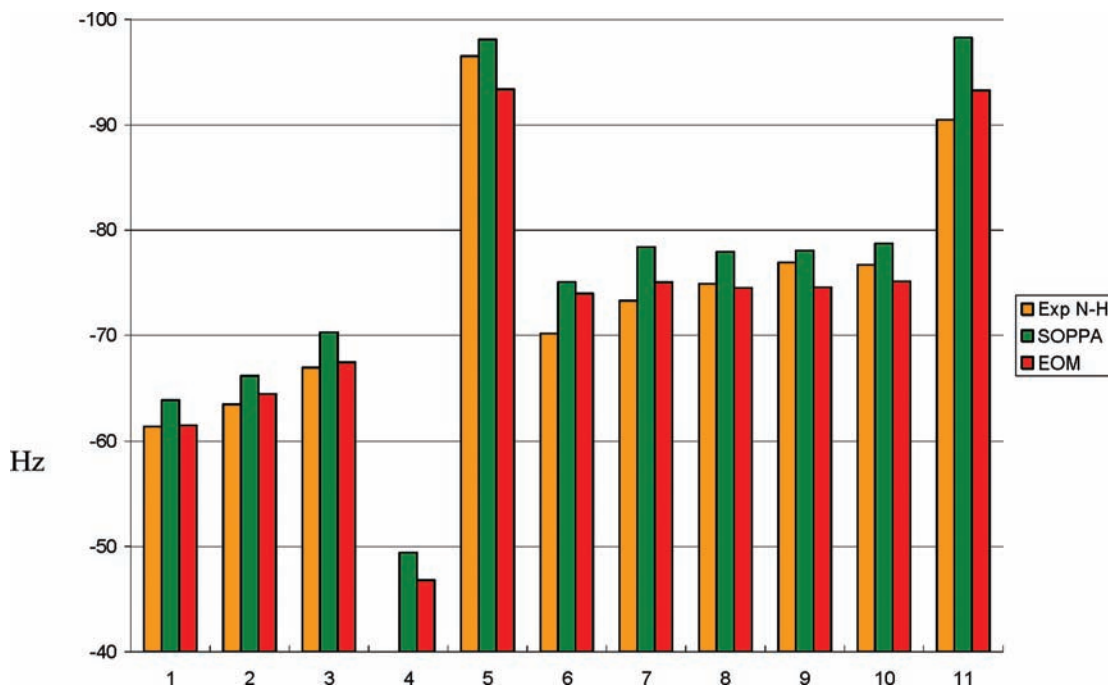


Figure 11. Bar graph comparing SOPPA, EOM-CCSD, and experimental $^1J(\text{N–H})$ values.

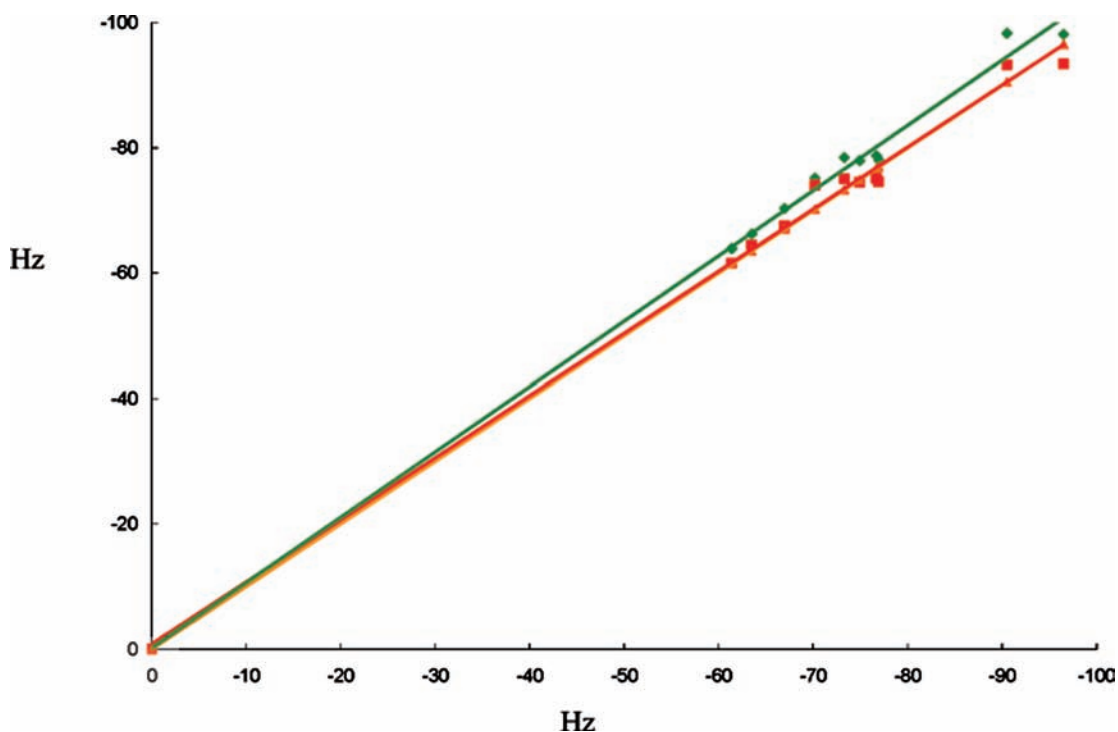


Figure 12. SOPPA (\blacklozenge , green line) and EOM-CCSD (\blacksquare , red line) $^1J(\text{N–H})$ vs experimental values and the reference trendline (\blacktriangle , orange line). A point at (0,0) has been added to both methods.

these atoms in larger chemical and biological systems which are not feasible for EOM-CCSD.

Acknowledgment. This paper is dedicated to our friend and colleague, Russ Pitzer, in recognition of his many contributions to chemistry and to the Ohio Supercomputer Center. J.E.D.B. is grateful to the Ohio Supercomputer Center for continuing support of this work. The Spanish team acknowledges financial support from the Ministerio de Ciencia y Tecnología (Project No. CTQ2007-61901/BQU) and Comunidad Autónoma de Madrid (Project MADRISOLAR, ref S-0505/PPQ/0225). Thanks are given to the CTI (CSIC) for allocation of computer time.

Supporting Information Available: Contains SOPPA and EOM-CCSD PSO, DSO, FC, and SD components of J for the molecules and ions investigated in this study and the full reference citations for refs 16, 26, and 27. This information is available free of charge via the Internet at <http://pubs.acs.org>.

References and Notes

- Del Bene, J. E.; Alkorta, I.; Elguero, J. *J. Chem. Theory Comput.* **2008**, *4*, 967.
- Del Bene, J. E.; Alkorta, I.; Elguero, J. *J. Chem. Theory Comput.* **2009**, *5*, 208.
- Herzberg, G. *Electronic spectra and electronic structure of polyatomic molecules*; Van Nostrand: New York, 1966; Appendix VI.
- Butcher, R. J.; Jones, W. J. *J. Mol. Spectrosc.* **1973**, *47*, 64.
- Harmony, M. D.; Laurie, V. W.; Kuczowski, R. L.; Schwendeman, R. H.; Ramsay, D. A.; Lovas, F. J.; Lafferty, W. J.; Maki, A. G. *J. Phys. Chem. Ref. Data* **1979**, *8*, 619.
- Winnewisser, M.; Cook, R. L. *J. Chem. Phys.* **1964**, *41*, 999.
- (a) Ruden, T. A.; Lutnæs, O. B.; Helgaker, T.; Ruud, K. *J. Chem. Phys.* **2003**, *118*, 9572. (b) Ruden, T. A.; Helgaker, T.; Jaszunski, M. *Chem. Phys.* **2004**, *296*, 53. (c) Ruden, T. A.; Ruud, K. Ro-vibrational corrections to NMR parameters In *Calculation of NMR and EPR Parameters*; Kaupp, M., Bühl, M., Malkin, V. G., Eds.; Wiley-VCH: Weinheim, 2004; p 153; (d) Helgaker, T.; Jaszunski, M.; Pecul, M. *Prog. Nucl. Magn. Reson. Spectrosc.* **2008**, *53*, 249.
- Pople, J. A.; Binkley, J. S.; Seeger, R. *Int. J. Quantum Chem. Quantum Chem. Symp.* **1976**, *10*, 1.
- Krishnan, R.; Pople, J. A. *Int. J. Quantum Chem.* **1978**, *14*, 91.
- Bartlett, R. J.; Silver, D. M. *J. Chem. Phys.* **1975**, *62*, 3258.
- Bartlett, R. J.; Purvis, G. D. *Int. J. Quantum Chem.* **1978**, *14*, 561.
- Hehre, W. J.; Ditchfield, R.; Pople, J. *J. Chem. Phys.* **1982**, *56*, 2257.
- Hariharan, P. C.; Pople, J. A. *Theor. Chim. Acta* **1973**, *28*, 213.
- Spitznagel, G. W.; Clark, T.; Chandrasekhar, J.; Schleyer, P. v. R. *J. Comput. Chem.* **1982**, *3*, 363.
- Clark, T.; Chandrasekhar, J.; Spitznagel, G. W.; Schleyer, P. v. R. *J. Comput. Chem.* **1983**, *294*.
- Frisch, M. J. et al. *Gaussian 03*; Gaussian, Inc.: Wallingford, CT, 2004.
- Enevoldsen, T.; Oddershede, J.; Sauer, S. P. A. *Theor. Chem. Acc.* **1998**, *100*, 275.
- (a) Geertsen, J.; Oddershede, J.; Scuseria, G. E. *J. Chem. Phys.* **1987**, *87*, 2138. (b) Oddershede, J.; Geertsen, J.; Scuseria, G. E. *J. Phys. Chem.* **1988**, *92*, 3056.
- (19) (a) Nielsen, E. S.; Jørgensen, P.; Oddershede, J. *J. Chem. Phys.* **1980**, *73*, 6238. (b) Oddershede, J.; Jørgensen, P.; Yeager, D. L. *Comput. Phys. Rep.* **1984**, *2*, 33.
- Packer, M. J.; Dalskov, E. K.; Enevoldsen, T.; Jensen, H. J. Aa; Oddershede, J. *J. Chem. Phys.* **1996**, *105*, 5886.
- Dalskov, E. K.; Sauer, S. P. A. *J. Phys. Chem. A* **1998**, *102*, 5269.
- Perera, S. A.; Sekino, H.; Bartlett, R. J. *J. Chem. Phys.* **1994**, *101*, 2186.
- Perera, S. A.; Nooijen, M.; Bartlett, R. J. *J. Chem. Phys.* **1996**, *104*, 3290.
- Schäfer, A.; Horn, H.; Ahlrichs, R. *J. Chem. Phys.* **1992**, *97*, 2571.
- Lynden-Bell, R. M.; Harris, R. K. *Nuclear Magnetic Resonance Spectroscopy*; Appleton Century Crofts: New York, 1969.
- Angeli, C. et al. *DALTON, a molecular electronic structural program*; Release 2.0, [ppt://www.kjemi.uio.no/software/dalton/dalton.htm](http://www.kjemi.uio.no/software/dalton/dalton.htm), 2005.
- Stanton, J. F. et al. *ACES II, a program product of the Quantum Theory Project*; University of Florida: Gainesville, FL.
- Antusek, A.; Dedziera, D.; Jackowski, K.; Jaszunski, M.; Makulski, W. *Chem. Phys.* **2008**, *352*, 320.
- Kalinowski, H.-O.; Berger, S.; Braun, S. *Carbon-13 NMR Spectroscopy*; John Wiley & Sons: Chichester, 1988; pp 495–508 and 549–571.
- Breitmaier, E.; Voelter, W. *¹³C NMR Spectroscopy*, 2nd ed.; Verlag Chemie: Weinheim, 1978; pp 106–108.
- Kamienska-Trela, K. One bond ¹³C–¹³C spin–spin coupling constants. In *Annual Reports on NMR Spectroscopy*; Webb, G. A., Ed.; Academic Press: Burlington, MA, 1995; Vol. 30, pp 130–230.
- Ruden, T. A.; Lutnæs, O. B.; Helgaker, T.; Ruud, K. *J. Chem. Phys.* **2003**, *118*, 9572.
- Halliday, J. D.; Bindner, P. E.; Padamshi, S. *Can. J. Chem.* **1984**, *62*, 1258.
- Berger, S.; Braun, S.; Kalinowski, H.-O. *NMR Spectroscopy of the Non-Metallic Elements*; John Wiley & Sons: Chichester, 1997; pp 245–274.
- Jackowski, K.; Wilczek, M.; Pecul, M.; Sadlej, J. *J. Phys. Chem. A* **2000**, *104*, 5955.
- Johnson, C. D. Pyridines and their benzo derivatives: Structure. In *Comprehensive Heterocyclic Chemistry II*; Katritzky, A. R., Rees, C. W., Scriven, E. F. V., Eds.; Pergamon: Oxford, 1996; Vol. 5, p 7.
- Palmer, M. H.; McNab, H.; Reed, D.; Pollacchi, A.; Walker, I. C.; Guest, M. F.; Siggel, M. R. F. *Chem. Phys.* **1997**, *214*, 191.
- Wilczek, M.; Kozminski, W.; Jackowski, K. *Chem. Phys. Lett.* **2002**, *358*, 263.
- Jimeno, M. L.; Alkorta, I.; Elguero, J.; Del Bene, J. E. *Magn. Reson. Chem.* **2006**, *44*, 698.
- Contreras, R. H.; Peralta, J. E. Angular dependence of spin-spin coupling constants. *Prog. Nucl. Magn. Reson. Spectrosc.* **2000**, *37*, 321.
- Varra, J.; Jokisaari, J.; Wasylishen, R. E.; Bryce, D. L. Spin-spin coupling tensors as determined by experiment and computational chemistry. *Prog. Nucl. Magn. Reson. Spectrosc.* **2002**, *41*, 233.
- Contreras, R. H.; Barone, V.; Facelli, J. C.; Peralta, J. E. Advances in Theoretical and Physical Aspects of Spin-Spin Coupling Constants. *Annu. Rep. NMR. Spectrosc.* **2003**, *51*, 167.
- Alkorta, I.; Elguero, J. *Int. J. Mol. Sci.* **2003**, *4*, 64.
- Helgaker, T.; Pecul, M. *Spin-Spin Coupling Constants with HF and DFT Methods, in Calculation of NMR and EPR Parameters*; Kaupp, M., Bühl, M., Malkin, V. G., Eds.; Wiley-VCH: Weinheim, 2004; p 101.
- Krivdin, L.; Contreras, R. N. Recent Advances in Theoretical Calculations of Indirect Spin-Spin Coupling Constants. *Annu. Rep. NMR Spectrosc.* **2007**, *61*, 133.
- Del Bene, J. E.; Elguero, J. *Magn. Reson. Chem.* **2007**, *45*, 484.
- Del Bene, J. E.; Elguero, J. *Solid State Nucl. Magn. Reson.* **2008**, *34*, 86.